Persistent Photoconductivity in Strontium Titanate

Marianne C. Tarun, Farida A. Selim, and Matthew D. McCluskey*

Department of Physics and Astronomy, Washington State University, Pullman, Washington 99164-2814, USA

(Received 8 May 2013; published 30 October 2013)

Persistent photoconductivity was observed in strontium titanate ($SrTiO_3$) single crystals. When exposed to sub-bandgap light (2.9 eV or higher) at room temperature, the free-electron concentration increases by over 2 orders of magnitude. After the light is turned off, the enhanced conductivity persists for several days, with negligible decay. From positron lifetime measurements, the persistent photoconductivity is attributed to the excitation of an electron from a titanium vacancy defect into the conduction band, with a very low recapture rate.

DOI: 10.1103/PhysRevLett.111.187403 PACS numbers: 78.56.−a, 71.55.−i

Complex oxides exhibit a range of novel physical phenomena including ferroelectricity, high-temperature superconductivity, and colossal magnetoresistance [1]. Strontium titanate ($SrTiO_3$), in particular, is the subject of intense fundamental and applied research efforts. The strong temperature and electric field dependence of its dielectric constant [2–4] leads to unusual electronic transport behavior [5,6]. $SrTiO_3$ is a wide-bandgap semiconductor (3.25 eV at room temperature [7]) with potential applications in oxide-based electronic devices [8,9]. By electron doping, the electrical properties of $SrTiO_3$ can be tuned from insulating to semiconducting, metallic, and even superconducting [10–12].

The $SrTiO_3/LaAlO_3$ interface often forms an electrically conductive layer, a surprising result explained in terms of the ''polar catastrophe'' [13,14]. In this model, the polar catastrophe is averted by electrons leaving the $LaAlO_3$ surface and accumulating at the interface. Alternatively, La donors may diffuse into $SrTiO_3$ and dope it *n* type [15–17]. It is possible that native defects play an important role in the conductive and photoconductive [18] properties of these interfaces. Specifically, cation vacancies [19–21] and their complexes with hydrogen [22,23] are present in bulk and thin film $SrTiO_3$.

In the present work, we annealed samples at high temperatures in order to produce vacancy defects. These annealed samples exhibit large persistent photoconductivity (PPC) at room temperature. While room-temperature PPC has been observed in wide-gap semiconductors such as GaN [24] and GaInNAs [25], the increase in conductivity is less than an order of magnitude. Below room temperature, point defects such as *DX* centers can lead to PPC [26,27]. First-principles calculations have shown that the *DX* center in GaAs involves the displacement of a donor atom from its substitutional site [28]. This large relaxation causes metastable behavior at low temperatures.

Verneuil-grown $SrTiO_3$ bulk single crystals were purchased from MTI Corporation [29]. Samples were sealed in an evacuated fused silica ampoule along with strontium oxide (SrO) powder and annealed at high temperature [30]. The annealing was conducted in a three-zone horizontal tube furnace at 1200° C for 1 h. After annealing, the ampoule was taken out of the furnace and allowed to cool to room temperature.

Measurements were performed at room temperature. Free-carrier absorption spectra were obtained using a Bomem DA8 vacuum Fourier transform infrared spectrometer with a globar light source, a KBr beam splitter, and a liquid-nitrogen-cooled InSb detector. Hall-effect measurements were performed in the van der Pauw geometry (MMR Technologies, Inc.). Melted indium was used to make electrical contacts. To explore the wavelength dependence of the photoconductivity, we utilized the 450-W Xe lamp of a spectrometer (JY-Horiba FluoroLog-3) as a source of monochromatic illumination.

An annealed sample was illuminated for 10 min at sub-bandgap wavelengths. After each light exposure, a free-carrier absorption spectrum was obtained. Figure 1 shows the change in absorbance at 3000 cm^{-1} (with the spectrum of the sample before illumination as a reference) as a function of illumination wavelength. The plot shows a threshold for photoconductivity at 430 nm (2.9 eV). The conductivity persists for days, indicating the presence of defects with metastable behavior [31]. PPC was not observed in as-received samples (Fig. 1).

To verify that the PPC is a bulk phenomenon, the front and back surfaces of an annealed sample were mechanically polished with 5-micron diamond lapping film. Free-carrier absorption spectra were obtained after illumination with a UV light emitting diode (wavelength 405 nm) for 30 min, with spectra before illumination as reference, for a polished and unpolished sample. As shown in Fig. 2, both samples show similar spectra, suggesting that the defects responsible for PPC are in the bulk rather than a near-surface layer. Since polishing can introduce defects, however, we also obtained a spectrum of an as-received sample that was mechanically polished. The lack of free-carrier absorption in that sample (Fig. 2) confirms that PPC is not caused by defects produced by mechanical polishing.

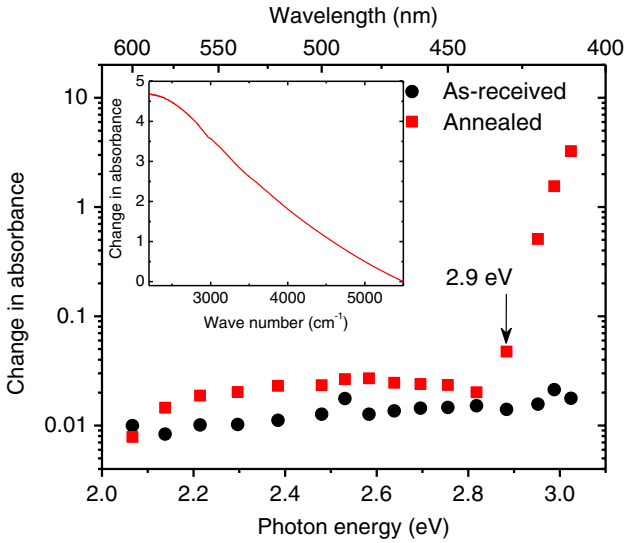

FIG. 1 (color online). Change in IR absorbance at 3000 cm^{-1} (reference: sample before illumination) at room temperature, as a function of illumination wavelength. Inset: Free-carrier absorption spectrum of the annealed sample after illuminating with a 415 nm light.

Hall-effect measurements were performed on the annealed sample before and after illumination at 410 nm for 30 min. Before illumination, the sample had an average electron carrier density of 5×10^{15} cm^{-3} and resistivity of 290 Ω cm (Fig. 3) [32]. After illumination, the carrier density increased to 2×10^{18} cm^{-3} while the resistivity dropped to 0.6 Ω cm. This photo-induced conductivity was monitored in the dark and was observed to persist for several days (Fig. 3).

To investigate the thermal properties of the PPC, the sample was heated in the Hall chamber under vacuum for 30 min at temperatures from 326 to 426 K. After each vacuum anneal, the sample was allowed to cool to room temperature and a Hall measurement was performed. As shown in Fig. 4, the carrier reduction is significant for higher annealing temperatures. The maximum annealing temperature (426 K) did not return the sample to its original low-carrier-density state before illumination. A full recovery likely requires a much higher annealing temperature, suggesting a thermal barrier to electron capture by the defect.

The decay in carrier density was simulated with a bimolecular model [33].

$$n = \frac{n_0}{1 + n_0 C t}, \tag{1}$$

where n is the electron density after annealing at temperature T, n_0 is the density prior to annealing at T, t is the annealing time (1800 s), and C is the capture rate. The capture rate is given by [31]

$$C = C_0 e^{-E_c/k_B T}, \tag{2}$$

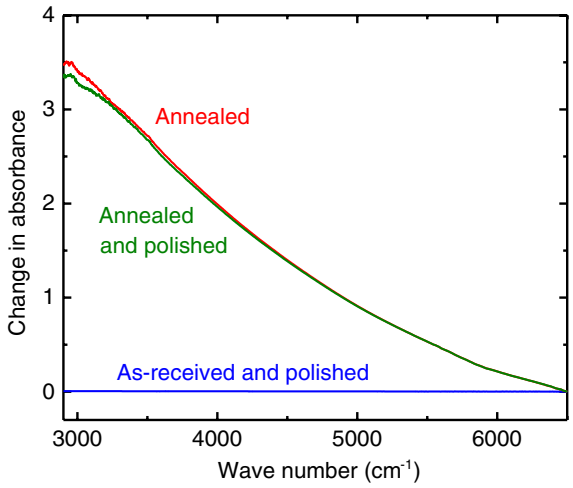

FIG. 2 (color online). Free-carrier absorption spectra at room temperature for samples exposed to 405 nm light (reference: sample before illumination).

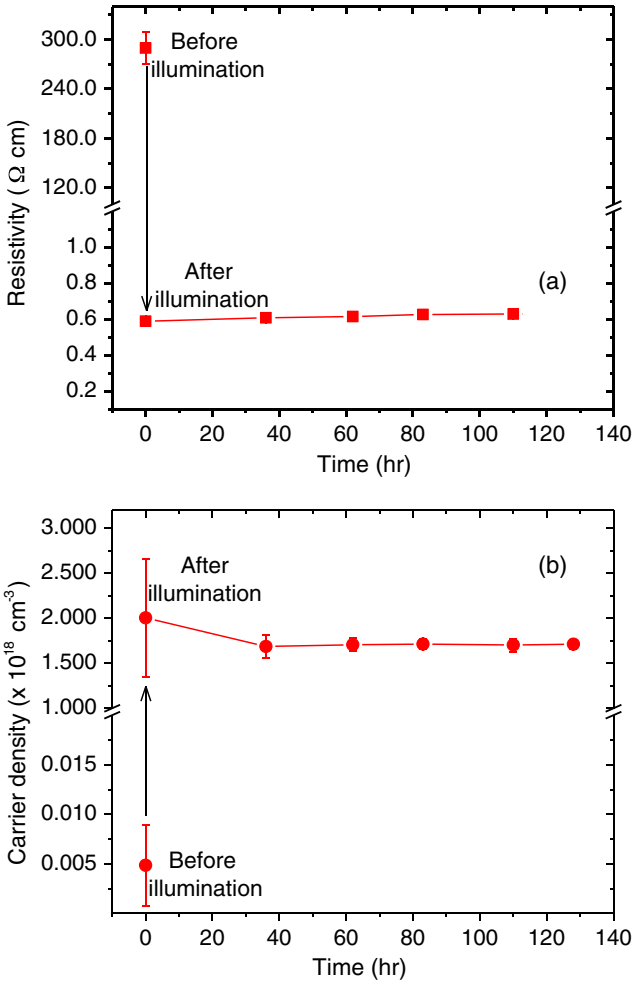

FIG. 3 (color online). (a) Resistivity and (b) carrier density of the annealed sample before and after illumination. After illumination, the sample was kept in the dark.

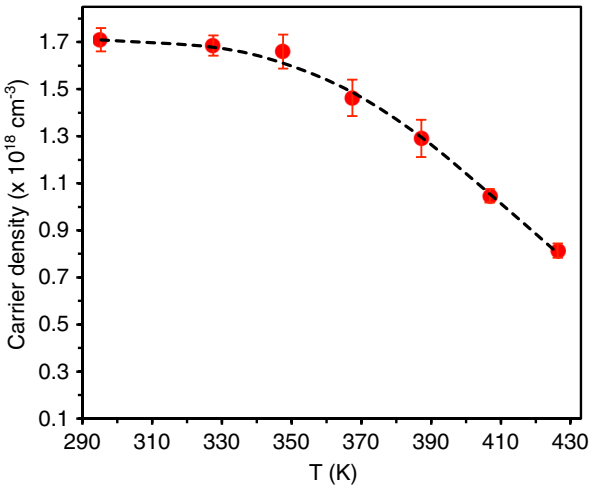

FIG. 4 (color online). Free-electron carrier density as a function of vacuum annealing temperature (the first data point is room temperature). The dashed line is a fit to Eqs. (1) and (2), which yields a capture barrier of 0.40 eV.

where C_0 is the capture rate at $T \rightarrow \infty$, E_c is the capture barrier, and k_B is the Boltzmann constant. Fitting the data to Eqs. (1) and (2) yields a capture barrier $E_c = 0.40$ eV (Fig. 4).

The effect of illumination and thermal annealing can be illustrated by a defect configuration-coordinate diagram [31], as shown in Fig. 5. In process 1, a photon of energy E_{opt} promotes an electron from the defect level to the conduction band. After photoexcitation, the defect relaxes into a metastable configuration. In process 2, the electron is recaptured, with a thermal barrier E_c. The defect must have enough thermal energy to surmount this capture barrier in order to return to its ground state.

To identify the defects responsible for PPC, positron lifetime measurements were carried out on as-received and annealed samples before and after illumination. Positron lifetime spectroscopy has been used to characterize vacancy defects in $SrTiO_3$ [19–21,34] as well as in other oxide materials such as ZnO [35,36]. In the present study, measurements were performed using a conventional fast-fast time coincidence spectrometer [37] with two BaF_2 γ-ray detectors mounted on photomultiplier tubes in collinear geometry, with an estimated time resolution of ~200 ps. The positron source ^{22}NaCl was deposited on an 8-μm thick Kapton support foil and was sandwiched between two identical samples. At least 7 million counts were collected in each measurement. The mean penetration depth of positrons emitted from the source is ~100 μm, which provides bulk measurements with negligible contribution from positron annihilation at the surface [38].

Lifetime spectra were analyzed as a superposition of exponential decay components convoluted with the instrumental timing resolution, which was fitted by three Gaussian functions [37]. Source correction due to positron annihilation in the source materials was taken into account in the fitting. Specifically, the Kapton foil introduces a decay component (10% of overall intensity) of 384 ps. This component was obtained by performing measurements on an annealed, defect-free Al calibration sample, and agrees with prior work [19]. The one defect simple trapping model [37,39] was used to analyze the data, using the PATFIT-88 program [40]. Figure 6 shows data with the Kapton foil component and constant background (~ 40 counts/channel) subtracted. The "before illumination" spectrum was multiplied by a normalization factor (1.13) so that both spectra have the same number of total counts. Parameters from the fits are listed in Table I.

The as-received sample shows a characteristic defect lifetime of 185 ps, which is consistent with Ti vacancies [19]. A Ti vacancy (V_{Ti}) is an acceptor and can have charge state of up to −4 [41], providing a strong positron trap. After annealing, the defect lifetime increased to 210 ps. This 210 ps defect lifetime may represent an unresolved average of V_{Ti} and Ti-O vacancy pairs ($V_{\text{Ti-O}}$), which have

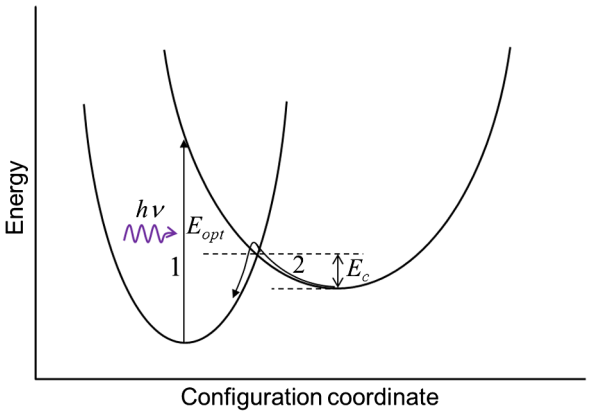

FIG. 5 (color online). Defect configuration-coordinate diagram describing (1) excitation of electron into conduction band and (2) electron recapture.

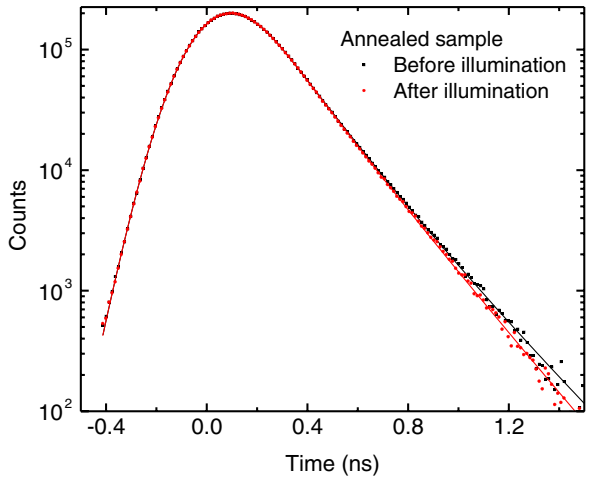

FIG. 6 (color online). Positron lifetime spectra of annealed sample before and after illumination.

TABLE I. Positron lifetime values (in ps) for as-received and annealed samples. The two lifetime components are given by τ_1 and τ_2, with respective annihilation fractions I_1 and I_2 ($I_1 + I_2 = 1$). The average lifetime τ_{ave} and trapping rate κ_d (in ps^{-1}) are also given.

$SrTiO_3$ sample	τ_1	τ_2	I_2 (%)	$\tau_{ave} = I_1\tau_1 + I_2\tau_2$	$\kappa_d = I_2(1/\tau_1 - 1/\tau_2)$
As-received	119.9(3.1)	185.1(3.0)	49.8(4.4)	152(9)	$1.5(0.2) \times 10^{-3}$
Annealed					
Before illumination	141.5(2.4)	209.6(6.2)	27.3(4.8)	160(12)	$0.6(0.1) \times 10^{-3}$
After illumination	125.8(3.5)	176.0(2.3)	58.7(5.3)	155(12)	$1.3(0.2) \times 10^{-3}$

calculated lifetime values of 184–195 ps and 225–239 ps, respectively [19]. We expect that annealing led to the formation of $V_{Ti\text{-}O}$ and probably also isolated oxygen vacancies (V_O), which do not trap positrons because of their +2 charge state. $V_{Ti\text{-}O}$ should have a less negative charge state (−2) than V_{Ti}, resulting in a decreased positron trapping rate, consistent with our observations. From these results, we conclude that $V_{Ti\text{-}O}$ is the defect responsible for PPC.

After illumination, the defect lifetime of the annealed sample decreased, while the trapping rate increased (Table I). The increase in trapping rate shows that more positron trapping at vacancies occurs after illumination. This means that some vacancies in the sample (e.g., isolated V_O) are converted to efficient positron traps by capturing electrons upon illumination, an effect that has been reported in GaAs [42]. The decrease in defect lifetime after illumination is attributed to (i) the reduction in the open volume of $V_{Ti\text{-}O}$, and (ii) the contribution of V_O, which has a shorter lifetime (166–178 ps) [19]. The combination of these two factors led to a substantial decrease in the measured defect lifetime, 176 ps, which is even smaller than the defect lifetime measured in the as-received sample.

In summary, room-temperature PPC has been observed in $SrTiO_3$, due to the excitation of an electron from a defect level to the conduction band. The findings highlight the role that defects play in determining the electrical properties of oxide materials. The discovery of PPC in $SrTiO_3$ could also lead to novel applications such as holographic memory.

The authors acknowledge C. Varney and J. Ji for assistance with positron lifetime measurements and M. Zafar Iqbal, A. Janotti, C. G. Van de Walle, and J. Varley for helpful interactions. This work was supported by NSF Grant No. DMR-1004804, with partial student support provided by DOE Grant No. DE-FG02-07ER46386. Positron lifetime measurements were supported by NSF Grant No. DMR-1066772.

*mattmcc@wsu.edu

[1] R. Ramesh and D. G. Schlom, MRS Bull. **33**, 1006 (2008).
[2] J. H. Barrett, Phys. Rev. **86**, 118 (1952).
[3] K. A. Müller and H. Burkard, Phys. Rev. B **19**, 3593 (1979).
[4] J. Hemberger, P. Lunkenheimer, R. Viana, R. Böhmer, and A. Loidl, Phys. Rev. B **52**, 13 159 (1995).
[5] A. Spinelli, M. A. Torija, C. Liu, C. Jan, and C. Leighton, Phys. Rev. B **81**, 155110 (2010).
[6] J. Son, P. Moetakef, B. Jalan, O. Bierwagen, N. J. Wright, R. Engel-Herbert, and S. Stemmer, Nat. Mater. **9**, 482 (2010).
[7] K. van Benthem, C. Elsässer, and R. H. French, J. Appl. Phys. **90**, 6156 (2001).
[8] K. Zhao, K. J. Jin, Y. H. Huang, S. Q. Zhao, H. B. Lu, M. He, Z. H. Chen, Y. L. Zhou, and G. Z. Yang, Appl. Phys. Lett. **89**, 173507 (2006).
[9] D. Kan, T. Terashima, R. Kanda, A. Masuno, K. Tanaka, S. Chu, H. Kan, A. Ishizumi, Y. Kanemitsu, Y. Shimakawa, and M. Takano, Nat. Mater. **4**, 816 (2005).
[10] J. F. Schooley, W. R. Hosler, and M. L. Cohen, Phys. Rev. Lett. **12**, 474 (1964).
[11] H. P. R. Frederikse, W. R. Thurber, and W. R. Hosler, Phys. Rev. **134**, A442 (1964).
[12] O. N. Tufte and P. W. Chapman, Phys. Rev. **155**, 796 (1967).
[13] A. Ohtomo and H. Y. Hwang, Nature (London) **427**, 423 (2004).
[14] S. Thiel, G. Hammerl, A. Schmehl, C. W. Schneider, and J. Mannhart, Science **313**, 1942 (2006).
[15] P. R. Willmott, S. A. Pauli, R. Herger, C. M. Schlepütz, D. Martoccia, B. D. Patterson, B. Delley, R. Clarke, D. Kumah, C. Cionca, and Y. Yacoby, Phys. Rev. Lett. **99**, 155502 (2007).
[16] A. S. Kalabukhov, Y. A. Boikov, I. T. Serenkov, V. I. Sakharov, V. N. Popok, R. Gunnarsson, J. Börjesson, N. Ljustina, E. Olsson, D. Winkler, and T. Claeson, Phys. Rev. Lett. **103**, 146101 (2009).
[17] S. A. Chambers, M. H. Engelhard, V. Shutthanandan, Z. Zhu, T. C. Droubay, L. Qiao, P. V. Sushko, T. Feng, H. D. Lee, T. Gustafsson, E. Garfunkel, A. B. Shah, J.-M. Zuo, and Q. M. Ramasse, Surf. Sci. Rep. **65**, 317 (2010).
[18] A. Tebano, E. Fabbri, D. Pergolesi, G. Balestrino, and E. Traversa, ACS Nano **6**, 1278 (2012).
[19] R. A. Mackie, S. Singh, J. Laverock, S. B. Dugdale, and D. J. Keeble, Phys. Rev. B **79**, 014102 (2009).
[20] D. J. Keeble, R. A. Mackie, W. Egger, B. Löwe, P. Pikart, C. Hugenschmidt, and T. J. Jackson, Phys. Rev. B **81**, 064102 (2010).
[21] D. J. Keeble, S. Wicklein, R. Dittmann, L. Ravelli, R. A. Mackie, and W. Egger, Phys. Rev. Lett. **105**, 226102 (2010).
[22] M. C. Tarun and M. D. McCluskey, J. Appl. Phys. **109**, 063706 (2011).
[23] J. T-Thienprasert, I. Fongkaew, D. J. Singh, M.-H. Du, and S. Limpijumnong, Phys. Rev. B **85**, 125205 (2012).

[24] M. T. Hirsch, J. A. Wolk, W. Walukiewicz, and E. E. Haller, Appl. Phys. Lett. **71**, 1098 (1997).
[25] J. Z. Li, J. Y. Lin, H. X. Jiang, J. F. Geisz, and S. R. Kurtz, Appl. Phys. Lett. **75**, 1899 (1999).
[26] D. V. Lang and R. A. Logan, Phys. Rev. Lett. **39**, 635 (1977).
[27] P. M. Mooney, J. Appl. Phys. **67**, R1 (1990).
[28] D. J. Chadi and K. J. Chang, Phys. Rev. Lett. **61**, 873 (1988).
[29] http://www.mtixtl.com/.
[30] SrO powder is necessary to suppress decomposition. Samples annealed with TiO_2 powder or in an Ar ambient showed heavy *n*-type conductivity, presumably related to oxygen vacancy formation.
[31] M. D. McCluskey and E. E. Haller, *Dopants and Defects in Semiconductors* (CRC Press, Boca Raton, FL, 2012).
[32] The sample was exposed to room light for several minutes to set up the electrical contacts.
[33] S. J. Jokela and M. D. McCluskey, Phys. Rev. B **72**, 113201 (2005).
[34] A. Gentils, O. Copie, G. Herranz, F. Fortuna, M. Bibes, K. Bouzehouane, É. Jacquet, C. Carrétéro, M. Basletić, E. Tafra, A. Hamzić, and A. Barthélémy, Phys. Rev. B **81**, 144109 (2010).
[35] F. Tuomisto, V. Ranki, K. Saarinen, and D. C. Look, Phys. Rev. Lett. **91**, 205502 (2003).
[36] F. A. Selim, M. H. Weber, D. Solodovnikov, and K. G. Lynn, Phys. Rev. Lett. **99**, 085502 (2007).
[37] R. Krause-Rehberg and H. S. Leipner, *Positron Annihilation in Semiconductors* (Springer-Verlag, Berlin, 1999).
[38] R. Krause-Rehberg and H. S. Leipner, *Positron Annihilation in Semiconductors* (Springer, New York, 1998), p. 10.
[39] F. Tuomisto and I. Makkonen, Rev. Mod. Phys. (to be published).
[40] P. Kirkegaard, N. J. Pedersen, and M. Eldrup, *PATFIT-88: A Data-Processing System for Positron Annihilation Spectra on Mainfraime and Personal Computers* (Risø National Laboratory, Grafisk Service, Risø, Denmark, 1989).
[41] E. Ertekin, V. Srinivasan, J. Ravichandran, P. B. Rossen, W. Siemons, A. Majumdar, R. Ramesh, and J. C. Grossman, Phys. Rev. B **85**, 195460 (2012).
[42] K. Saarinen, S. Kuisma, P. Hautojärvi, C. Corbel, and C. LeBerre, Phys. Rev. Lett. **70**, 2794 (1993).